Proximity between Nucleotide/Dinucleotide and Metal Ion Binding Sites in DNA-Dependent RNA Polymerase from *Escherichia coli*†

Suresh C. Tyagi*

Department of Biochemistry and Cell Biology, State University of New York at Stony Brook, Stony Brook, New York 11794-5215

Received October 9, 1991; Revised Manuscript Received February 28, 1992

ABSTRACT: In order to understand translocation in transcription, it is important to develop a continuous functional assay for RNA polymerase (RNAP) activity in vitro. Fluorescent derivatives of ATP, UTP, UpA, and CpA with aminonaphthalene-5-sulfonic acid (AmNS) attached to the nucleotide triphosphates via a γ-phosphoramidate bond or to the dinucleotide monophosphates via a 5′-secondary amine linkage were synthesized [Tyagi, S. C., & Wu, F. Y.-H. (1987) *J. Biol. Chem. 262*, 10684–10688]. The fluorescent emission spectra of (5′-AmNS)UpA, (5′-AmNS)CpA, (γ-AmNS)ATP, and (γ-AmNS)UTP overlap the absorption spectrum of co-substituted RNA polymerase (Co-RNAP) and ensure fluorescence resonance energy transfer (FRET) between the fluorescent analog and Co(II) in Co-RNAP. The binding constants at a single site for (γ-AmNS)ATP, (γ-AmNS)UTP, (5′-AmNS)UpA, and (5′-AmNS)CpA were observed to be 7.11, 5.26, 0.52, and 0.61 μM, respectively, in Co-RNAP and 5.70, 3.42, 0.12, and 0.21 μM, respectively, in Zn-RNAP. (8-AmTEMPO)ATP, with the spin probe AmTEMPO attached to the C-8 position at ATP [Tyagi, S. C. (1991) *J. Biol. Chem. 266*, 17936–17940], and Mn(3′-OCH_3)UTP were synthesized. Mn(II)-substituted RNA polymerase (Mn-RNAP) is prepared. The single site binding constants for (8-AmTEMPO)ATP and Mn(3′-OCH_3)UTP were 3.58 and 2.35 μM in Zn-RNAP and 5.77 and 3.43 μM in Mn-RNAP, respectively. These results indicate that dinucleotides bind much more tightly than mononucleotides to RNAP and that the binding constants are roughly the same for both Co- and Zn-substituted RNAP. FRET distances were found to be 16.6, 16.8, 17.7, and 14.4 Å between the binding sites for (γ-AmNS)ATP, (γ-AmNS)UTP, (5′-AmNS)UpA, and (5′-AmNS)CpA, respectively, and the Co(II) in the β-subunit of RNAP. Steady-state kinetic measurements on the incorporation of these analogs into RNA indicate that binding between substrate and RNAP becomes looser in the presence of DNA and other components of RNA synthesis. This indicates that these analogs undergo some alteration during catalysis.

Transcription by RNA polymerase (RNAP)[1] is a complex process which involves (1) promoter recognition and subsequent DNA template binding to RNAP; (2) ribonucleotide binding; (3) formation of the first phosphodiester bond (initiation); (4) translocation of the enzyme and product; (5) subsequent binding and addition of ribonucleotides (elongation); and (6) RNA chain termination. Each of these processes consists of several substeps (Chamberlin, 1974; Hawley & McClure, 1983; von Hippel et al., 1984; McClure, 1985). It has been postulated that many of these steps are accompanied by conformational changes and translocation of the enzyme and product (Chamberlin, 1974; McClure, 1985). However, precise experimental docomentation of these alterations is limited.

Prokaryotic RNA polymerase (RNAP) is more highly purified than many eukaryotic RNAP (Burgess & Jendrisak, 1975). RNAP from *Escherichia coli* is an oligomeric enzyme ($\alpha_2\beta\beta'\sigma$) (Chamberlin, 1982; Lewis & Burgess, 1982). On the basis of an electron microscopy study, a model of *E. coli* RNA polymerase in three-dimensional space has been predicted (Darst et al., 1989). Another significance of studying *E. coli* RNAP as a model for RNAP from higher eukaryotes is that the largest subunits of prokaryote and eukaryote RNAP have considerable homology in their primary amino acid sequences (Allison et al., 1985; Bigg et al., 1985; Broyles & Moss, 1986; Sweetser et al., 1987; Aheam et al., 1987). Also, the σ subunit of bacterial RNAP has considerable similarity to eukaryotic transcription factors (Helman & Chamberlin, 1988; Jaehning, 1991). It seems likely that essential features of the catalytic mechanism of RNA polymerase are also conserved across species. Therefore, in order to understand the molecular mechanism of transcription, the structure, function, and regulation of RNAP from *E. coli* are the focus of many laboratories (Chamberlin, 1974; Roeder, 1976; Kumar, 1981; McClure, 1985; Chuknyisky et al., 1990; Johnson et al., 1991; Yager & von Hippel, 1991) including our own (Tyagi & Wu, 1987; Wu & Tyagi, 1987; Tyagi, 1991). In order to understand the general mechanism of transcription by RNA polymerase, we have been attempting to investigate translocation steps in transcription by developing a continuous assay for RNAP activity by spectroscopic methods. The enzyme contains two zinc ions per molecule of enzyme (Scrutton et al., 1971), the substrate binding subunit, β, and the DNA template binding subunit, β′, each containing one metal ion (Miller et al., 1979). In addition, this enzyme possesses two

† This work was supported in part by National Institutes of Health Grants GM28057 and HL14262.

* Corresponding address: Department of Medicine, Division of Cardiology, University of Missouri, Columbia, MO 65212.

[1] Abbreviations: RNAP, RNA polymerase; AmNS, 1-aminonaphthalene-5-sulfonic acid; (5′-AmNS)UpA, 5′-[1-(5-sulfonic acid)-naphthylamino]uridylyl(3′,5′)adenosine; (5′-AmNS)CpA, 5′-[1-(5-sulfonic acid)naphthylamino]cytidylyl(3′,5′)adenosine; (γ-AmNS)ATP, adenosine 5′-triphosphoro-γ-1-(5-sulfonic acid)naphthylamidate; (γ-AmNS)UTP, uridine-5′-triphosphoro-γ-1-(5-sulfonic acid)naphthyl amidate; TLC, thin-layer chromatography; EPR, electron paramagnetic resonance; FRET, fluorescence resonance energy transfer; β-ME, β-mercaptoethanol; EDTA, ethylenediaminetetraacetic acid; poly(dA-dT), double-stranded alternating copolymer of deoxyadenylate–thymidylate; DTT, dithiothreitol; Mn(3′-OCH_3)UTP, manganese(II) 3′-methoxyuridine 5′-triphosphate; (8-AmTEMPO)ATP, 8-amino-(2,2,6,6-tetramethylpiperidinyl-*N*-oxy)adenosine 5′-triphosphate.

0006-2960/92/0431-6447$03.00/0

substrate binding sites, the initiation and the elongation site (Wu & Goldthwait, 1969a; 1969b). The initiation site preferentially binds purine nucleotides (Maitra & Hurwitz, 1965) or dinucleotide monophosphate in which the 5′-terminal base is either adenine or guanine (Downey & So, 1970).

Previously we have reported the synthesis and characterization of dinucleoside monophosphates, e.g., (5′-AmNS)-UpA/CpA, and mononucleoside triphosphates, e.g., (γ-AmNS)ATP/UTP, containing the fluorophore, 1-amino-(5-sulfonic acid)naphthyl linked at the 5′-terminus and γ-phosphorus, respectively (Tyagi & Wu, 1987). These fluorescence substrate analogs have their emission maxima around 445 and 464 nm, respectively, when excited at 340 nm. These emission spectra overlap the absorption spectrum of Co-substituted RNAP (Co-RNAP), and FRET distance measurements have been employed to demonstrate no significant changes in the distances between the nucleotide and dinucleotide binding sites and the intrinsic metal ion in the β subunit of RNAP in the presence or absence of DNA (Wu & Tyagi, 1987). However, a marked increase in the fluorescence of initiator [(5′-AmNS)UpA] and elongator [(γ-AmNS)UTP] analogs, respectively, was observed upon addition of subsequent nucleotide substrates for RNA synthesis (Wu & Tyagi, 1987). Also, we have synthesized spin-labeled analogs of ATP and UTP (Tyagi, 1991) and showed that additional information on the catalytic sites in RNAP can be obtained by examining the structure and conformation of bound nucleotides by fluorescence and EPR techniques.

In this paper we report the catalytic and the physical binding and the FRET distance measurements of dinucleotide and mononucleotide analogs to RNAP. The binding constants and the steady-state kinetic parameters of incorporation of these analogs into RNA were estimated. We have shown that RNAP has reduced affinity for these analogs during catalysis of RNA polymerization (in the presence of DNA and other substrates), indicating that these analogs and RNAP undergo some alteration during catalysis and can be used as probes to measure the RNAP activity continuously.

Materials and Methods

Materials. Nucleoside triphosphates (NTPs), dinucleoside monophosphates (diNMPs), and poly(dA-dT) were obtained from P-L Biochemicals. [^{3}H]UTP and [^{3}H]ATP were from ICN Pharmaceuticals. Tris was from Schwarz/Mann. Calf thymus DNA (type I, highly polymerized) was obtained from Bio-Rad. All other chemicals and biochemicals were of highest purity and were obtained commercially.

Enzyme. The DNA-dependent RNA polymerase from *E. coli* MRE-600 cells (Grain Processing Co., Muscatine, IL) was purified by the method of Burgess and Jendrisak (1975). The enzyme was at least 98% pure as judged by NaDodSO$_4$–polyacrylamide gel electrophoresis and was stored at −20 °C in a buffer containing 50 mM Tris–HCl (pH 7.8), 50% glycerol, 0.15 M NaCl, 0.1 mM EDTA, and 0.1 mM DTT. The enzyme concentration was determined by the extinction coefficient ($\epsilon^{1\%}_{280nm}$) of 6.2 (Lowe et al., 1979), and by the Bio-Rad dye binding assay (Bradford, 1976).

Metal-Substituted RNA Polymerase. The selective substitution of metal ion in the β subunit of RNAP was carried out according to our previously reported method (Wu & Tyagi, 1987). Subunit separation into $\alpha_2\beta$ and β′ from core RNAP (Wu, et al., 1971) and metal content determination in the subunit was estimated as described previously (Wu & Tyagi, 1987).

Substrate Analogs. Fluorescent analogs of mononucleoside triphosphates, (γ-AmNS)ATP and (γ-AmNS)UTP, were prepared as described by Yarbrough et al. (1979). The synthesis and structural characterization of (5′-AmNS)UpA and other AmNS derivatives of dinucleoside monophosphates were carried out according to our previous report (Tyagi & Wu, 1987). The synthesis and spectroscopic properties of spin-labeled nucleotide substrate analogs have been reported recently (Tyagi, 1991).

Synthesis of Mn(3′-OCH$_3$)UTP. Two milligrams (11 mM) of MnSO$_4$ and 5 mg (8.6 mM) of sodium salt of (3′-OCH$_3$)UTP were dissolved in 1 mL of buffer A (50 mM Tris-HCl (pH 7.5), 0.1 M NaCl, and 0.1 mM EDTA). The solution was stirred for 2.5 h at 60 °C. The mixture was passed through a Sephadex G-25F column (1.5 × 55 cm), equilibrated with the same buffer. The sample was eluted with buffer A, and the A_{260nm} of fractions was recorded. The peak fractions in the elution profile were collected and concentrated. The Mn content of the concentrated fractions was determined by atomic absorption spectroscopy. The purity of the compound was checked by thin-layer chromatography (TLC). The compound was used within an hour after synthesis without further separating into stereoisomers.

Biochemical Assay. The enzymatic activity of RNAP and metal-substituted RNAP was assayed by incorporation of ^{3}H-labeled ribonucleoside monophosphate into acid-insoluble material using calf thymus DNA or poly(dA-dT) as a template (Burgess, 1969). The enzyme assay mixture (0.25 mL) for studying the utilization of mononucleoside triphosphates and their fluorescent analogs contained 1.675 μg of RNAP, 50 mM Tris-HCl (pH 7.9), 5 mM MgCl$_2$, 0.1 mM β-ME, 10 μg of DNA, 0.4 mM each CTP, GTP, [^{3}H]ATP (1565 cpm/nmol), and (γ-AmNS)UTP or Mn(3′-OCH$_3$)UTP. No GTP and CTP were added when poly(dA-dT) was used as DNA template. MgCl$_2$ was omitted from the reaction buffer when Mn(3′-OCH$_3$)UTP was used as the substrate. [^{3}H]UTP (2442 cpm/nmol) was employed as the marker when (γ-AmNS)-ATP or (8-AmTEMPO)ATP was used as the substrate analogs. The concentration of substrate analogs was varied from 2 to 400 μM. The mixtures were incubated for 10 min at 37 °C. The acid-precipitable [^{3}H]RNA product was collected on Whatman GF/A filters and counted in a liquid scintillation counter.

Spectroscopy. Absorption spectra were recorded in 1-cm quartz cuvettes using a Perkin-Elmer Lambda 3B UV/vis spectrophotometer interfaced with a Perkin-Elmer 3600 data station. All fluorescence excitation and emission spectra were recorded at 1-nm intervals on a computer-controlled Spex Datamate spectrofluorometer and corrected for the buffer base line and instrument response. The excitation and emission slits were adjusted for 5-nm band pass width. Micro cells (0.3 × 0.3 cm, 120 μL) were used for all the experiments. EPR spectra were recorded at room temperature with a Varian E-4 spectrophotometer (X-band at 9.05 GHz) at 22 ± 1 °C. Aqueous samples of 25–50 μL were placed in quartz capillary tubing of 1 mm width, and the end of the tubing was closed by using polyethylene tubing and a Teflon plug. Spectra were recorded at a modulation amplitude of 0.5 G with a 100-kHz modulation frequency, a microwave power of 1 mW, a time constant of 1 s, and a scan time of 4 min. The fluorescence and EPR records were averaged over at least five determinations. Samples were prepared and incubated for 10 min before their spectra were recorded. All spectroscopic measurements were carried out at 37 °C in a temperature-controlled cuvette holder.

Binding Studies. The binding constants for fluorescent analogs to RNAP were estimated from fluorescence quenching

of substrate analogs at 445 or 464 nm for (5′-AmNS)-UpA/CpA and (γ-AmNS)ATP/UTP (0.1 μM), respectively when excited at 340 nm in the presence of Co-RNAP. The concentration of Co-RNAP or Zn-RNAP was varied from 0.1 to 25 μM. The binding constants of enzyme-spin-labeled substrate complexes were determined by observing the change in the X-band EPR absorption intensity at low field for (8-AmTEMPO)ATP (6 μM) or Mn(3′-OCH_3)UTP (5 μM) upon addition of Mn-RNAP or Zn-RNAP. The concentration of Mn-RNAP or Zn-RNAP was varied from 2 to 35 μM in 50 mM Tris-HCl (pH 7.9), 5 mM $MgCl_2$ [no $MgCl_2$ was used for Mn(3′-OCH_3)UTP], 50 mM KCl, and 0.1 mM β-ME.

Corrections to Fluorescence and EPR Data. Fluorescence and EPR intensities were corrected for absorption due to Co(II) in Co-RNAP and Mn(II) in Mn-RNAP in the fluorescence and EPR spectra, respectively, using the relationship (Brand & Witholt, 1967)

$$I_{corr} = I_{obsd}\frac{2.3AL}{(1 - 10^{-A})L}$$

where A refers to the optical density of solution measured at excitation wavelength with a light path, L (1 cm), for the fluorescence measurements. A in the EPR measurements is the intensity at low field due to intrinsic Mn(II) in Mn-RNAP.

Fraction of Bound Ligand. The fluorescence and EPR intensities of a enzyme–ligand mixture, in which total enzyme concentration [E_o] and total ligand concentration [S_o] are known, allow the calculation of the concentrations of all three components at equilibrium. We have calculated the fraction of ligand bound (f) by taking the fluorescence or EPR intensities of a mixture of free ligand [S] and ligand bound to enzyme [E·S] as the sum of the yields of its components, given by

$$f = (I_s - I_f)/(I_b - I_f)$$

where I_s, I_f, and I_b are the fluorescence or EPR intensity of ligand–enzyme mixture, total free ligand, and total bound ligand, respectively. From f we find [E·S] by the relationship [E·S] = f[S_o].

The $K_d = 1/K_a$ of the enzyme–substrate complex were calculated according to the Scatchard (1949) equation:

$$\frac{[E\cdot S]}{[S_o]([E_o] - [E\cdot S])} = K_a N - K_a\frac{[E\cdot S]}{[S_o]}$$

where N is number of binding sites.

Results

Steady-State Kinetic Studies. We have measured the initial velocity (v = [^{3}H]NMP incorporated per minute per nanomole of RNAP) for fluorescent and spin-labeled analogs at various concentrations of analogs. The dependence of initial velocity on the substrate analog concentration was plotted. The kinetic parameters for the formation of oligonucleotide catalyzed by poly(dA-dT)-directed RNA polymerase with analogs of substrate were calculated and compared to the unmodified substrate. The kinetic mechanism for the reaction of preequilibrated complex of enzyme (E), DNA template (D), and nucleotide substrate (N), with various concentrations of substrate analog (S) can be represented by the Scheme I. The following equation can be derived from Scheme I, when [N] ≫ K_{EN} and [D] ≫ K_{ED}:

$$V\,(min^{-1}) = \frac{k_3K_i[S]}{K_{EDNS} + K_{EDNS}K_i[S] + K_i[S]}$$

where $K_i = (1/K_{ES} + 1/K_{EDS} + 1/K_{ENS})$.

Under the experimental conditions, where [N] ≫ K_{ENS} and [D] ≫ K_{EDS} and E in [E·S] is negligible, then Scheme I can be reduced to the Michaelis–Menten kinetic scheme given in Scheme II. The measured K_{EDNS} refered to dissociation constant for [S] from EDNS complex. The calculated values of K_{EDNS} and k_3 are reported in Table I.

Scheme I

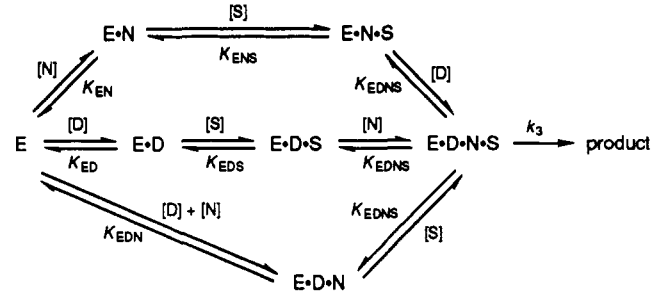

Scheme II

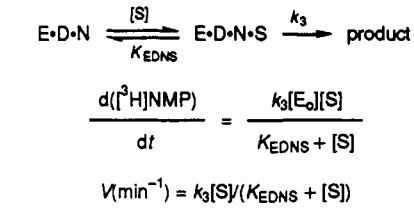

Table I: Steady-State Kinetic Constants of Fluorescence and Spin-Labeled Substrates for DNA-Dependent RNA Polymerase from *E. coli*[a]

nucleotide	K_{EDNS} (μM)	k_3 (min^{-1})
ATP	11.76 ± 0.37	4.83 ± 0.10
(8-AmTEMPO)ATP	21.57 ± 0.34	4.67 ± 0.09
UTP	16.30 ± 0.04	3.20 ± 0.02
(γ-AmNS)UTP	27.66 ± 0.17	1.76 ± 0.01
(3′-OCH_3)UTP	34.76 ± 0.14	1.49 ± 0.01
Mn(3′-OCH_3)UTP	5.31 ± 0.21	0.88 ± 0.02
UpA	0.85 ± 0.05	1.66 ± 0.01
(5′-AmNS)UpA	4.01 ± 0.11	2.62 ± 0.03

[a] Reaction mixture (0.25 mL) contained RNA polymerase (1.675 μg) and 54 nM poly(dA-dT) (based on 702-bp-long template) in 50 mM Tris-HCl (pH 7.9), 5 mM $MgCl_2$ (no $MgCl_2$ was added when Mn(3′-OCH_3)UTP was used as substrate), and 0.1 mM β-ME. UpA or (5′-AmNS)UpA was varied from 2 to 400 μM in the presence of 0.4 mM ATP and [^{3}H]UTP (2442 cpm/nmol). ATP or (γ-AmNS)ATP was varied from 2 to 400 μM in the presence of 0.4 mM [^{3}H]UTP (2442 cpm/nmol). UTP or (γ-AmNS)UTP or (3′-OCH_3)UTP or Mn(3′-OCH_3)UTP was varied from 2 to 400 μM in the presence of 0.4 mM [^{3}H]ATP (1565 cpm/nmol). Samples were incubated at 37 °C, precipitated with 5% TCA and filtered on GF/C paper. The radioactivity was measured.

Fluorescence Studies. The fluorescence emission and excitation spectra of nucleotide and dinucleotide analogs were recorded. Analogs of NTPs emit at 465 nm, and diNMPs emit at 445 nm when both are excited at 340 nm. This emission overlaps with the 395- and 465-nm absorption bands of Co-substituted RNAP (Figure 1). The Co-substituted RNAP (Co-RNAP) is 91% active as compared to the reconstituted Zn-RNAP. The content of Co(II) in RNAP was found to be 1 mol of Co(II)/mol of enzyme. The subunit location of the Co(II) in the reconstituted RNAP was determined by chromatography of the urea-treated core ($\alpha_2\beta'\beta$) RNAP on an Affi-Gel blue column as described by Wu et al. (1971) and by atomic absorption analyses of the metal ion content in the $\alpha_2\beta$ subcomplex and β' subunit. The results showed that the substituted Co(II) was incorporated into the β subunit of RNAP since the α subunit does not contain any bound metals (Wu et al., 1971). We have employed the emission quenching of analogs by Co-RNAP and by Zn-RNAP to calculate the

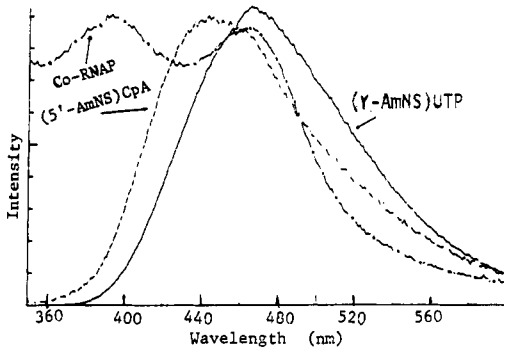

FIGURE 1: Spectral overlap relationship between three moieties of two energy donor–acceptor pairs. Emission spectra of (5′-AmNS)CpA and (γ-AmNS)UTP, in 50 mM Tris-HCl (pH 7.9), 50 mM KCl, 10 mM $MgCl_2$, 0.1 mM EDTA, 0.1 mM DTT, and 5% glycerol at 25 °C with excitation at 340 nm. (5′-AmNS)CpA (---); (γ-AmNS)UTP (—). The absorption spectrum of Co-RNAP (-·-) shows a maximum at 460 nm (ϵ = 2400 M^{-1} cm^{-1}).

Table II: Dissociation Constant (K_d) of Enzyme–Substrate Complex, Quantum Yield (Q_d), Energy Transfer Efficiency (E), Spectral Integral Overlap (J), Distance at 50% Probability (R_o), and Distance (r) between Bound Substrate Analog and Co(II) in the β Subunit in the RNA Polymerase of *E. coli*[a]

analog	K_d[b] (μM)	Q_d	E	$J \times 10^{-15}$ (M^{-1} cm^3)	R_o (Å)	r (Å)
(γ-AmNS)ATP	7.11 (5.70)	0.420	0.96	8.60	28.6	16.6
(γ-AmNS)UTP	5.26 (3.42)	0.086	0.83	8.44	21.9	16.8
(5′-AmNS)UpA	0.52 (0.12)	0.071	0.75	8.75	21.3	17.7
(5′-AmNS)CpA	0.61 (0.21)	0.037	0.84	8.39	19.0	14.4

[a] The samples contained 0.1 μM substrate analog and 20 μM RNA polymerase in 10 mM Tris-HCl (pH 8), 0.1 mM EDTA, and 0.1 mM β-ME. [b] K_d values in the bracket are for Zn-RNAP. $E = 1 - (F_{Co\text{-}RNAP}/F_{Zn\text{-}RNAP})$. $R_o = 9790(k^2 Q_d \eta^{-4} J)^{1/6}$; where $k^2 = 2/3$ and $\eta^{-4} = 0.26$. $r = R_o[(1 - E)/E]^{1/6}$.

binding constants. (5′-AmNS)UpA (0.1 μM) was titrated with various concentrations of Zn-RNAP or Co-RNAP. The maximal quenching of (5′-AmNS)UpA fluorescence by enzyme at saturation was 80% for Co-RNAP and 15% for Zn-RNAP. The emission at 445 nm was recorded as a function of RNAP concentrations. The intensities were corrected for inner-filter effects. A Scatchard plot for (5′-AmNS)UpA binding to Co-RNAP and Zn-RNAP is shown in Figure 2. The binding constants (K_d) for (γ-AmNS)ATP, (γ-AmNS)UTP, (5′-AmNS)UpA, and (5′-AmNS)CpA to Co-RNAP and Zn-RNAP are reported in Table II.

FRET (Forster, 1948; Stryer, 1978; Beechem & Brand, 1985) was employed to calculate the distances between fluorescent analogs and Co(II) in the β subunit of RNAP. The quantum yields (Q_d) of samples were determined by recording the corrected emission spectra of the reference standard and sample. In order to minimize the changes in the Q_d of fluorescent analog upon binding to RNAP, we have incubated fluorescent analogs with Zn-RNAP before their emission spectra were recorded. Zn-RNAP binds to these analogs but cannot quench emission through energy transfer. The Q_d of the sample was calculated according to the following equation (White et al., 1960; Melhuish, 1962; Chen, 1965):

$$Q_d = Q_s \frac{\int F_d \Delta\lambda}{\int F_s \Delta\lambda} \frac{q_s}{q_d} \frac{A_s}{A_d}$$

The subscript s and d refer to standard and unknown, respectively. F is the fluorescence intensity and Δλ is the wavelength interval over which the integration was carried out (Δλ is 1 nm in this case). q equals the relative photon output of the source at the excitation wavelength, taken directly from

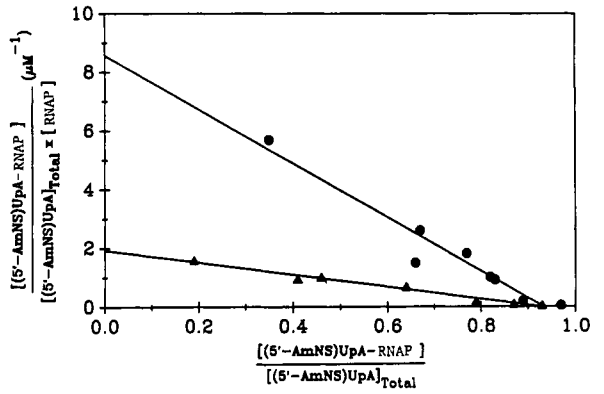

FIGURE 2: Scatchard plots for (5′-AmNS)UpA binding to RNA polymerase measured by fluorescence spectroscopy: Fluorescence titration of 0.1 μM (5′-AmNS)UpA with varying concentrations (0.1–25 μM) of Zn-RNAP (●) or Co-RNAP (▲) in buffer containing 50 mM Tris-HCl (pH 7.9), 0.1 mM β-ME, 50 mM KCl, and 5 mM $MgCl_2$. Band-pass slits were 5 nm for both excitation and emission wavelengths. Lines are the linear least-squares fit to all data points.

the calibration curve since the slits were kept constant. A is the absorbance at the excitation wavelength. Solutions with the absorbance at either excitation or emission wavelength < 0.01 were used for measurements to reduce the inner-filter effect. The respective Q_d for (γ-AmNS)ATP, for (γ-AmNS)UTP (λ_{ex} = 340 nm; λ_{em} = 465 nm), and for (5′-AmNS)UpA, (5′-AmNS)CpA (λ_{ex} = 340 nm; λ_{em} = 445 nm), in 10 mM Tris–HCl (pH 8) were determined using quinine sulfate in 0.1 N H_2SO_4 as the standard (Q_s = 0.55) (Drushel et al., 1963). The values of quantum yield for (γ-AmNS)ATP, (γ-AmNS)UTP, (5′-AmNS)UpA, and (5′-AmNS)CpA are reported in Table II. The spectral integral overlap was calculated by the following equation:

$$J\ (M^{-1}\ cm^3) = \frac{\int F_d(\lambda)\ \epsilon_a(\lambda)\ \lambda^4\ \Delta\lambda}{\int F_d(\lambda)\ \Delta\lambda}$$

where $F_d(\lambda)$ and $\epsilon_a(\lambda)$ are the relative fluorescence intensity (%) of the donor in the presence of Zn-RNAP and the molar extinction coefficient (M^{-1} cm^{-1}) of the acceptor (Co-RNAP), respectively. λ is the wavelength in nanometers. The summation was taken at 1-nm intervals, Δλ. On the basis of the binding constants for Co-RNAP, we have calculated the fraction of bound substrate on the enzyme during FRET and corrected the energy transfer efficiency (E). Modification of a computer program (Wu & Tyagi, 1987) was used to calculate Q_d, J, R_o, E, and r values (Table II).

EPR Studies. The spin-labeled analog of UTP, Mn(3′-OCH_3)UTP, was synthesized. The purity of this complex was checked on TLC on Whatman 3 MM paper. The compound migrated as a single spot under UV light. Atomic absorption analysis showed a Mn content of 0.8 ± 0.1 mol/mol of Mn-(3′-OCH_3)UTP. This indicates that a single Mn(II) is most likely associated with the phosphates as shown in MnATP complexes by X-ray crystallography (Sabat et al., 1985). On the basis of the perturbation in the low-field region of EPR signal from $MnSO_4$ upon addition of (3′-OCH_3)UTP, we have estimated the dissociation constant of Mn(3′-OCH_3)UTP to be ~1 μM. The dissociation constant (K_d) for $MgATP^{2-}$ was observed to be 13 μM (O'Sullivan & Perrin, 1964). This may indicate that Mn(II) binds about 10 times tighter than Mg(II) to the nucleotides.

EPR spectra for (8-AmTEMPO)ATP, Mn(3′-OCH_3)UTP, and Mn(II)-substituted RNA polymerase (Mn-RNAP) were recorded. (8-AmTEMPO)ATP has a standard three-line

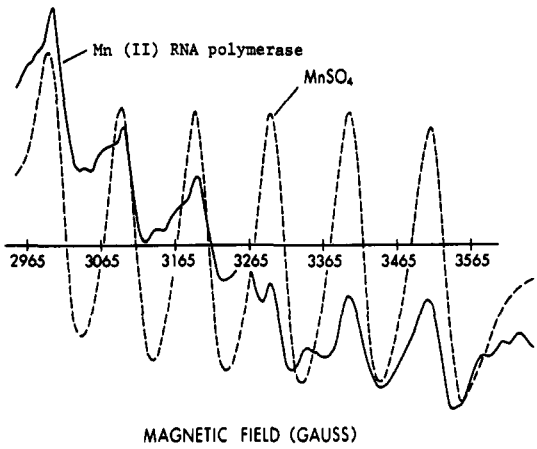

FIGURE 3: EPR spectrum of Mn(II)-RNAP (—): The fractional Mn(II) content in the enzyme is 0.9 ± 0.1 (mol/mol of enzyme). The concentration of Mn(II)-RNAP is 25 μM. The reference EPR spectrum of $MnSO_4$ (---) under the same conditions is shown. Buffer contained 50 mM Tris-HCl (pH 7.5), 0.1 M NaCl, and 0.1 mM EDTA. Instrument settings: time constant, 1 s; modulation amplitude, 0.5 G at 100-kHz modulation frequency; gain, 10^4 for $MnSO_4$ and 10^5 for Mn(II)-RNAP, respectively; microwave power, 1.0 mW; microwave frequency, 9.05 GHz; and scan time, 4 min at 24 ± 1 °C.

Table III: Dissociation Constant (K_d) and Number of Binding Sites (N) of Spin-Labeled Substrate Analogs for DNA-Dependent RNA Polymerase from *E. coli*[a]

RNA polymerase	analog	K_d (μM)	N
Zn-RNAP	(8-AmTEMPO)ATP	3.58 ± 0.04	1.21 ± 0.05
Mn-RNAP	(8-AmTEMPO)ATP	5.77 ± 0.02	1.23 ± 0.02
Zn-RNAP	Mn(3′-OCH_3)UTP	2.35 ± 0.05	1.06 ± 0.11
Mn-RNAP	Mn(3′-OCH_3)UTP	3.43 ± 0.06	1.03 ± 0.01

[a] (8-AmTEMPO)ATP (6 μM) and Mn(3′-OCH_3)UTP (5 μM) were titrated with varying (2–35 μM) concentrations of Zn-RNAP or Mn-RNAP in buffer containing 50 mM Tris-HCl (pH 7.9), 50 mM KCl, 0.1 mM β-ME, and 5 mM $MgCl_2$ (no $MgCl_2$ was added when Mn(3′-OCH_3)UTP was used as the titrant). Instrument settings were as follows: time constant, 1 s; modulation amplitude, 0.5 G; gain, 5 × 10^4; microwave power, 1.0 mW; scan time, 4 min; modulation frequency, 100 kHz; microwave frequency, 9.05 GHz (X-band); and temperature, 22 ± 1 °C.

spectrum (Tyagi, 1991), whereas Mn(3′-OCH_3)UTP gives rise to a six-line Mn(II) spectrum. A similar EPR spectrum has been reported for $MnATP^{2-}$ (Chapman et al., 1977). Mn-RNAP was prepared similarly as reported for Co-RNAP. The activity of Mn-RNAP was 95% of that of Zn-RNAP. Subunit localization indicated that Mn(II) was confined in the β subunit in RNAP. The EPR spectrum of Mn-RNAP is shown in Figure 3. The decrease in the amplitude of the low-field portion of the EPR spectrum for both types of analogs, (8-AmTEMPO)ATP and Mn(3′-OCH_3)UTP, was recorded as a function of Zn-RNAP or Mn-RNAP concentrations, respectively. The Scatchard plots for Mn(3′-OCH_3)UTP binding to Zn-RNAP and Mn-RNAP are shown in Figure 4. The dissociation constants (K_d) for (8-AmTEMPO)ATP are 3.58 and 5.77 μM, and for Mn(3′-OCH_3)UTP they are 2.35 and 3.43 μM, for Zn-RNAP and Mn-RNAP, respectively (Table III).

Discussion

We have utilized fluorescent and spin-labeled analogs in RNA synthesis and indicated that the binding of these analogs to RNA polymerase is altered during several steps in transcription.

The binding constant for ATP in the absence of divalent metal ion was reported to be 100 μM; this binding site was

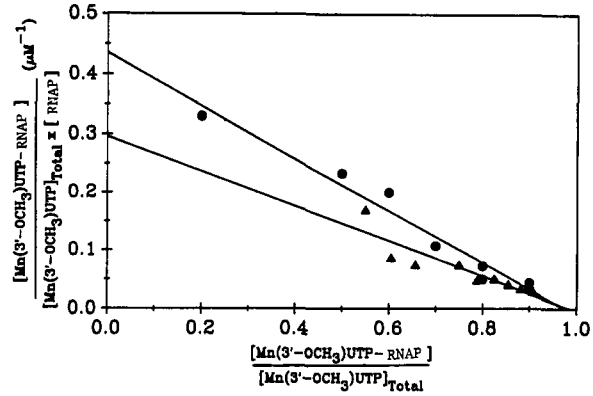

FIGURE 4: Scatchard plots for Mn(3′-OCH_3)UTP binding to RNA polymerase measured by EPR spectroscopy: EPR titration of 5 μM Mn(3′-OCH_3)UTP with varying concentrations (2–35 μM) of Zn-RNAP (●) or Mn-RNAP (▲) in buffer containing 50 mM Tris-HCl (pH 7.5), 0.1 M NaCl, and 0.1 mM EDTA. Instrument settings: time constant, 1 s; modulation amplitude, 0.5 G at 100-kHz modulation frequency; gain, 5 × 10^4; microwave power, 1.0 mW; microwave frequency, 9.05 GHz (X-band); and scan time, 4 min at 24 ± 1 °C. Lines are the linear least-squares fit to all data points.

assigned as the initiation site on the enzyme (Wu & Goldthwait, 1969a,b). Binding of ATP and UTP becomes tighter (10 μM) in the presence of Mg(II) ion; this was assigned to the elongation site on the enzyme (Wu & Goldthwait, 1969a,b). Downey and So (1970) observed binding for both ATP and UTP (=20 μM) and concluded that ATP binds at the initiation site whereas as UTP in the presence of divalent metal ion binds at the elongation sites. Rhodes and Chamberlin (1974) determined the binding constants of MgATP and MgUTP on poly(dA-dT)-directed RNA polymerase to be 7 and 16 μM, respectively, at the initiation and elongation sites.

The constants, K_{EDNS}, for ATP, UTP, and their analogs determined under steady-state conditions were in the range of 12–35 μM. The values of the constants for their physical binding to RNAP in the absence of turnover were in the range of 3–7 μM as measured by fluorescence and EPR methods. This indicates that enzyme–substrate complexes becomes less tight in the presence of DNA and nucleotide substrates. This may be explained if one considers the turnover of enzyme for catalysis for the second molecule of the substrate. However, the value of the turnover rate constant of the enzyme, k_3 (min^{-1}), does not change significantly for modified and unmodified substrate analogs (Table I). This indicates that these analogs are good substrates for RNA polymerase. Also, the values of k_3 for our substrate analogs were in agreement with the value of the turnover rate constant (=1.98, min^{-1}) for RNA polymerase on T7 DNA template observed by Prosen and Cech (1986). On the other hand, we observed a difference in k_3 for the dinucleotides UpA and (5′-AmNS)UpA. In Table I, the value of k_3 for UpA is 1.66. This value was higher for (5′-AmNS)UpA (2.62). This may suggest that a caplike structure on the 5′ end of the RNA product may induce elongation of RNA with a higher efficiency than that of the unmodified dinucleotide.

Previously, we have indicated that AmNS, at the 5′-end of UpA, is lying above the plane of the adenine ring and may float freely giving rise to the fluorescence enhancement (Wu & Tyagi, 1987).

The binding constant for dinucleotide on RNAP was <1 μM as compared to the value for nucleoside triphosphates which is in the range of 3–7 μM. It is possible that stacking of the bases in the dinucleotide increases its affinity toward RNA polymerase.

It has been shown that RNAP binds nucleotides much more tightly in the presence of divalent metal ion (Koren & Mildvan, 1977), which is also involved in the elongation of RNA product. In other enzymes, it has been shown that $MgATP^{2-}$ is a good substrate for ATP-dependent kinases (Storer & Cornish-Bowden, 1977) whereas free Mg(II) is actually an inhibitor and not an activator (indeed Mg-free ATP^{4-} is another inhibitor and not a substrate). Furthermore, the activity of bacteriophage T7 DNA polymerase was more efficient when Mn^{2+} rather than Mg^{2+} was used in buffer for the catalysis of DNA synthesis (Tabor & Richardson, 1989, 1990). We observed tighter binding of Mn(3′-OCH_3)UTP than of (3′-OCH_3)UTP. Similar results have been reported for complexes of Mn(II) and Mg(II) ions with other nucleotide substrates (Steck et al., 1968; Armstrong et al., 1979). The binding constant of free Mn(II) to RNA polymerase was estimated to be about 10 μM (Koren & Mildvan, 1977). We observed the binding constant of Mn(II) to (3′-OCH_3)UTP to be about 1 μM. This indicates that at a concentration of Mn(3′-OCH_3)UTP of 5 μM very little Mn(II) will be free as opposed to tied up in the Mn(3′-OCH_3)UTP complex.

The distance measurements based on FRET for (γ-AmNS)ATP and (γ-AmNS)UTP from Co(II) in the β subunit in RNAP were found to be in the same range for both nucleotide analogs, (γ-AmNS)ATP and (γ-AmNS)UTP. However, the distances for (5′-AmNS)UpA and (5′-AmNS)CpA were apparently different. (5′-AmNS)UpA seems to be about 3.3 Å further away than (5′-AmNS)CpA, from the Co(II) in the β subunit in RNAP (Table II). This may indicate that the analogs may still bind to RNAP via adenosine base moiety but the fluorophore conformation in CpA is more stacked as compared to UpA.

EPR Spectra of Mn(II)-RNAP. EPR spectra of Mn-$(H_2O)_6^{2+}$ and Mn(II)-RNAP are shown in Figure 3. The spectrum of the Mn-hexaaquo complex shows the standard six lines due to the interaction of the electron spin moment with the nucleus ($I = {}^5/_2$). The Mn(II)-hexaaquo cation is perfectly symmetrical, isotropically averaged with coordination environment, superimposed five electron–electron fine structure transitions with the six electronic energy levels resulting from the d^5 configuration. The coordination sphere around Mn(II) in the aquo complex is cubically symmetric, and the tumbling time for this small complex is sufficiently fast to average any environmental anisotropies. On the other hand, the anisotropy present in Mn(II)-RNAP spectra (Figure 3) is consistent with the possibility that Mn^{2+} may bind more strongly to the ligands (S, N, and O) in the RNAP as compared to the solvent molecules in aquo complex. This strong interaction of Mn(II) with ligands in RNAP may introduce rigidity in the electronic environment and consequently will introduce some anisotropy in the spectrum. Furthermore, the EPR spectra of Mn(II)-RNAP shows anisotropy in four to five hyperfine lines and isotropy in one to two lines (Figure 3). It is possible that four to five positions of Mn(II) innersphere coordination are taken by the ligands from the enzyme, whereas one to two positions may still be coordinating with an OH or water molecule to exchange ligand or substrate molecule during catalysis.

We have shown that the physical binding of substrate analogs to RNA polymerase becomes looser in the presence of DNA and other nucleotide substrate indicating that these analogs and RNA polymerase undergo alteration during transcription. These observations have prompted us to study further the process of translocation of enzyme and product by fast kinetic approaches. Stopped-flow studies utilizing these fluorescent substrate analogs and metal-hybrid RNA polymerase are in progress. We have determined binding constants for two spin-labeled nucleotides on the basis of the perturbation in the EPR absorption line arising from the interactions between two paramagetic probes, i.e., Mn(II) in RNAP and in Mn(3′-OCH_3)UTP and AmTEMPO in (8-AmTEMPO)ATP. Dipole–dipole hyperfine line broadening studies on these analogs should provide more information on the interactions of Mn-RNAP and spin-labeled nucleotides. Such studies are also in progress.

Acknowledgments

I thank Dr. Sanford R. Simon for his critical review of the manuscript.

References

Ahaem, J. M., Bartoiomei, M. S., West, M. L. Clsek, L. J., & Corden, J. L. (1987) *J. Biol. Chem. 262*, 10695–10705.
Allison, L. A., Moyle, M., Shales, M., & Ingles, C. (1985) *Cell 42*, 599–610.
Armstrong, R. N., Kondon, H., Granot, J., Kaiser, E. T., & Mildvan, A. S. (1979) *Biochemistry 18*, 1230–1238.
Beechem, J. M., & Brand, L. (1985) *Annu. Rev. Biochem. 54*, 43–71.
Bigg, J., Searles, L. L., & Greenleaf, A. (1985) *Cell 42*, 611–621.
Bradford, M. M. (1976) *Anal. Biochem. 72*, 248–254.
Brand, L., & Witholt, B. (1967) *Methods Enzymol. 11*, 776–856.
Broyles, S. S., & Moss, B. (1986) *Proc. Natl. Acad. Sci. U.S.A. 83*, 3141–3145.
Burgess, R. R. (1969) *J. Biol. Chem. 244*, 6160–6167.
Burgess, R. R., & Jendrisak, J. J. (1975) *Biochemistry 14*, 4634–4645.
Chamberlin, M. J. (1974) *Annu. Rev. Biochem. 43*, 721–775.
Chamberlin, M. J. (1982) *Enzymes 15*, 61–86.
Chapman, B. E., O'Sullivan, W. J., Scopes, R. K., & Reed, G. H. (1977) *Biochemistry 16*, 1005–1010.
Chen, R. F. (1965) *Science 150*, 1593–1595.
Chuknyisky, P. P., Rifkind, J. M., Tarien, E., Beal, R. B., & Eichhorn, G. L. (1990) *Biochemistry 29*, 5987–5994.
Darst, S. A., Kubalek, E. W., & Kornberg, R. D. (1989) *Nature 340*, 730–732.
Downey, K. M., & So, A. G. (1970) *Biochemistry 9*, 2520–2525.
Drushel, H. V., Sommers, A. L., & Cox, R. C. (1963) *Anal. Chem. 35*, 13–21.
Forster, T. (1948) *Ann. Phys. 2*, 55–75.
Hawley, D. K., & McClure, W. R. (1983) *Nucleic Acids Res. 11*, 2237–2255.
Helman, J. D., & Chamberlin, M. J. (1988) *Annu. Rev. Biochem. 57*, 839–872.
Jaehning, J. A. (1991) *Science 253*, 859.
Johnson, R. S., Boweres, M., & Eaton, Q. (1991) *Biochemistry 30*, 189–198.
Koren, R., & Mildvan, A. S. (1977) *Biochemistry 16*, 241–249.
Kumar, S. A. (1981) *Prog. Biophys. Mol. Biol. 38*, 165–210.
Lewis, M. K., & Burgess, R. R. (1982) *Enzymes (3rd Ed.) 15*, 109–153.
Lowe, P. A., Hager, D. A., & Burgess, R. R. (1979) *Biochemistry 18*, 1344–1352.
Maitra, U., & Hurwitz, J. (1965) *Proc. Natl. Acad. Sci. U.S.A. 54*, 815–822.
McClure, W. R. (1985) *Annu. Rev. Biochem. 54*, 171–204.
Melhuish, W. H. (1962) *J. Opt. Soc. Am. 52*, 1256–1258.

Miller, J. A., Serio, G. F., Howard, R. A., Bear, J. L., Evans, J. E., & Kimball, A. P. (1979) *Biochim. Biophys. Acta 579*, 291-297.
O'Sullivan, W. J., & Perrin, D. D. (1964) *Biochemistry 3*, 18-26.
Prosen, D. E., & Cech, C. L. (1986) *Biochemistry 25*, 5378-5387.
Rhodes, G., & Chamberlin, M. J. (1974) *J. Biol. Chem. 249*, 6675-6683.
Roeder, R. G. (1976) in *RNA Polymerase* (Losick, R., & Chamberlin, M., Eds.) pp 285-329, Cold Spring Harbor Laboratory, Cold Spring Harbor, NY.
Sabat, M., Cini, R., Harmony, T., & Sundaralingam, M. (1985) *Biochemistry 24*, 7827-7833.
Scatchard, C. T. (1949) *Ann. N.Y. Acad. Sci. 51*, 660-672.
Scrutton, M. C., Wu, C.-W., & Goldthwait, D. A. (1971) *Proc. Natl. Acad. Sci. U.S.A. 68*, 2497-2501.
Steck, T. L., Caicuts, M. J., & Wilson, R. G. (1968) *J. Biol. Chem. 243*, 2769-1778.
Storer, A. C., & Cornish-Bowden, A. (1977) *Biochem. J. 165*, 61-69.
Stryer, L. (1978) *Annu. Rev. Biochem. 47*, 819-846.
Sweetser, D., Nonet, M., & Young, R. A (1987) *Proc. Natl. Acad. Sci. U.S.A. 84*, 1192-1196.
Tabor, S., & Richardson, C. C. (1989) *Proc. Natl. Acad. Sci. U.S.A. 86*, 4076-4080.
Tabor, S., & Richardson, C. C. (1990) *J. Biol. Chem. 265*, 8322-8328.
Tyagi, S. C. (1991) *J. Biol. Chem. 266*, 17936-17940.
Tyagi, S. C., & Wu, F. Y.-H. (1987) *J. Biol. Chem. 262*, 10684-10688.
von Hippel, P. H., Bear, D. G., Morgan, W. D., & McSwiggen, J. A. (1984) *Annu. Rev. Biochem. 54*, 389-446.
White, C. E., Ho, M., & Weimer, E. Q. (1960) *Anal. Chem. 32*, 438-440.
Wu, C.-W., & Goldthwait, D. A. (1969a) *Biochemistry 8*, 4450-4458.
Wu, C.-W., & Goldthwait, D. A. (1969b) *Biochemistry 8*, 4458-4464.
Wu, C. W., Wu, F. Y.-H., & Speckhard, D. C. (1971) *Biochemistry 16*, 5449-5454.
Wu, F. Y.-H., & Tyagi, S. C. (1987) *J. Biol. Chem. 262*, 13147-13154.
Yager, T. D., & von Hippel, P. H. (1991) *Biochemistry 30*, 1097-1118.
Yarbrough, L. R., Schlageck, J. G., & Maughman, M. (1979) *J. Biol. Chem. 254*, 12069-12073.

A ^{1}H-NMR Study of the DNA Binding Characteristics of Thioformyldistamycin, an Amide Isosteric Lexitropsin†

Malvinder P. Singh,‡ Surat Kumar,‡ Tomi Joseph,‡ Richard T. Pon,§ and J. William Lown*,‡
Department of Chemistry, University of Alberta, Edmonton, Alberta T6G 2G2, Canada, and Regional DNA Synthesis Laboratory, University of Calgary, Calgary, Alberta T2N 4N1, Canada
Received December 20, 1991; Revised Manuscript Received April 15, 1992

ABSTRACT: The interaction of thioformyldistamycin, an amide isostere of the naturally occurring antibiotic distamycin A, with a self-complementary decadeoxynucleotide duplex, d(CGCAATTGCG)$_2$, has been examined using a variety of high-field ^{1}H-NMR techniques. The ligand exhibits two forms in solution arising from geometric isomerism due to restricted rotation around the thioformamide bond. Only the thermodynamically more stable *Z*-form is shown to bind to the oligonucleotide along its minor groove at the central 5′-AATT segment with the end groups of the ligand extending into the flanking GC regions but without any close contact at the amidinium terminus. Cross-peaks involving characteristic intra- and interresidue proton connectivities in the 2D experiments (COSY and NOESY) were employed to assign individual resonances of both strands in the asymmetric DNA–drug complex. The solution structure of the complex was constructed by molecular mechanics calculations based upon initial estimates of drug–DNA NOE contacts and further refined through energy minimization. These results complement previous structural studies on distamycin and other lexitropsins with oligonucleotides. The exchange of the ligand between two equivalent binding sites on the DNA sequence was estimated to occur at 40 s^{-1} with a free energy of activation of 16.5 kcal·mol^{-1} at 321–326 K. There was no evidence of formation of a 2:1 drug–oligomer complex, in contrast to the case of the natural product, which is attributed to steric demands of the larger sulfur atom.

Several compounds including distamycin A (Arcamone et al., 1967; Hahn, 1975), netropsin (Julia & Preau-Joseph, 1963), anthelvencin A (Probst et al., 1965), noformycin (Diana, 1973), and the kikumycins A and B (Takahishi et al., 1972) comprise the pyrrole amidine class of antitumor antibiotics. These oligopeptides appear to share a common molecular mechanism of binding to double-stranded B-DNA (Wartell et al., 1974) and are known to inhibit the DNA and RNA polymerase activity in vitro through interactions with the DNA template, thereby blocking the synthesis of DNA (Hahn, 1980; Zimmer et al., 1971, 1983). Both distamycin A and netropsin have been of widespread interest in biochemical and biophysical investigations, and the reader is directed to extensive reviews on such studies (Hahn, 1980;

† This investigation was supported by a grant (to J.W.L.) from the National Cancer Institute of Canada.
* Address correspondence to this author.
‡ University of Alberta.
§ University of Calgary.

0006-2960/92/0431-6453$03.00/0